Low-Level Cloud Motion Winds from Meteosat High-Resolution Visible Imagery

ANDREAS OTTENBACHER

European Space Agency/European Space Operations Centre, Darmstadt, Germany

MARIA TOMASSINI

European Centre for Medium-Range Weather Forecasts, Reading, Berkshire, United Kingdom

KENNETH HOLMLUND AND JOHANNES SCHMETZ

European Organisation for Meteorological Satellites, Darmstadt, Germany

23 April 1996 and 7 October 1996

ABSTRACT

Low-level wind fields over the Atlantic have been derived from clouds in Meteosat high-resolution visible images experimentally with one production cycle per day over a period of more than 1 yr. The cloud motion winds from VIS imagery (VIS-CMW) use a template size of 32 × 32 VIS pixels, corresponding to about 80 km × 80 km at the subsatellite point, which is four times better than for the corresponding IR (infrared window) winds (160 km × 160 km). The yield is increased through the better spatial resolution of the VIS images and a better contrast between cloud and ocean surface, which effectively leads to an increase in wind vectors by a factor of 6. This implies a much better description of the low-level atmospheric flow by the VIS-CMW as compared to IR winds. The impact of the new VIS-CMW has been tested with a data assimilation experiment at the European Centre for Medium-Range Weather Forecasts, and small positive improvements have been found. The mean vector rms difference versus the verifying analysis shows improvement by up to 15% over some areas of the Atlantic Ocean. Comparisons of the short-term forecast using VIS cloud motion winds with independent scatterometer surface winds confirm the small improvements.

1. Introduction

Wind fields derived from tracking cloud motions in successive satellite infrared (IR: 10.5–12.5 μm) images have been produced routinely since the early 1970s from U.S. geostationary satellites (Leese et al. 1971; Hubert and Whitney 1971). They have become the most important product derived from geostationary meteorological satellites and they are an important data source for numerical weather prediction (NWP) (e.g., Radford 1989; Thoss 1992; Kelly 1992). To date, cloud motion winds (CMWs) from the tracking of IR channel images are operationally produced from U.S., Japanese, Indian, and European satellites. Algorithms used to derive wind speed and altitude from the radiance observations are well documented by, for example, Kelkar and Rao (1992), Le Marshall et al. (1994), Merrill et al. (1991), Nieman et al. (1993), Schmetz et al. (1993), and Uchida (1992).

The tracking of cloudy features in IR images is augmented by the use of the water vapor channel (WV: 5.7–7.1 μm) (Stewart et al. 1985; Laurent 1993). The use of the WV absorption channel has advantages over the IR window channel as tracers are more numerous due to the better sensitivity of the WV channel to thin clouds and moisture features. Water vapor winds from Meteosat are an operational product disseminated to users via the Global Telecommunication System (Holmlund 1993). Velden et al. (1992) show that, in particular, WV winds help to improve the forecasting of hurricane tracks.

The use of the Meteosat visible channel (VIS: 0.4–1.1 μm) for the tracking of cloudy features has been limited so far to experimental studies mainly related to tropical storm analysis. The VIS channels have much better spatial resolution than the IR channel. On Meteosat the VIS resolution at the subsatellite point is 2.5 km × 2.5 km as opposed to 5 km × 5 km for the IR, while the VIS on the U.S. Geostationary Operational Environmental Satellite (GOES) and the Japanese Geostationary Meteorological Satellite (GMS) has a spatial resolution as good as 1 km × 1 km and 1.25 km × 1.25 km, respectively. Rodgers et al. (1979) studied the wind fields around tropical cyclones using IR and VIS and found that full-resolution VIS images are needed to track slow-moving cloud elements. Rodgers et al. also

Corresponding author address: Dr. Johannes Schmetz, EUMETSAT, Am Kavalleriesand 31, D-64295 Darmstadt, Germany.
E-mail: schmetz@eumetsat.de

realized that the full advantage of high-resolution VIS tracking emerged only with the use of short interval scans (7.5 min). Uchida et al. (1991) derived low-level cloud motion winds from the VIS channel of the Japanese GMS satellite in the vicinity of typhoons. They studied the utility of different time intervals between successive images (7.5, 15, and 30 min) and concluded that shorter intervals are required in order to track low-level winds close to the typhoon center. Reed et al. (1988) also emphasized the need for, and value of, low-level winds over the Atlantic in the vicinity of easterly waves and incipient hurricanes.

This study focuses on the high-resolution aspect of VIS images from Meteosat. Low-level clouds are tracked in successive high-resolution VIS images (2.5 km $\times$ 2.5 km) over all ocean areas within the Meteosat field of view. Since this is being done in a quasi-operational mode, the standard time interval of 30 min between successive images is retained. The study shows that the VIS tracking provides a more complete description of the large-scale low-level flow as compared to IR low-level CMWs and also depicts circulation features of smaller scale. The impact of the new high-resolution VIS CMWs on NWP is shown through tests with the forecast model of the European Centre for Medium-Range Weather Forecasts (ECMWF).

2. Cloud motion winds from VIS images

a. Image data

The geostationary Meteosat satellites view the earth with an imaging radiometer in three channels: in the solar spectrum (VIS) between 0.4 and 1.1 μm, in the IR window region between 10.5 and 12.5 μm, and in the WV absorption band between 5.7 and 7.1 μm. Images are taken at half-hourly intervals, and the spatial sampling at the subsatellite point corresponds to 2.5 km $\times$ 2.5 km for the VIS and 5 km $\times$ 5 km in the IR and WV channels. In this study the derivation of CMWs uses VIS images for the cloud tracking. The IR channel is used for the height attribution of wind vectors.

A Meteosat VIS image (Fig. 1) clearly depicts the abundant fields of stratocumulus over the South Atlantic that constitute the lion's share of the useful tracers. Noteworthy also is Tropical Storm (hurricane) Noel at low latitudes in the North Atlantic. Figure 2 shows the corresponding image of the IR channel that is currently used for the operational derivation of winds at all levels. It is interesting to note that the contrast between low clouds and sea surface is much lower in the IR than in the VIS since the temperature difference between sea surface and low-level cloud is only a few dg kelvins. The superior contrast in the VIS images suits low-level cloud tracking better than the IR image data.

b. Tracer selection

The first step in the production of VIS CMWs is a multispectral image analysis (Tomassini 1981; Schmetz et al. 1993), which extracts the dominant features (sea, land, or clouds at different levels) in an image segment corresponding to an area of 32 $\times$ 32 IR pixels. An area is selected for the cloud tracking if, first, the segment is over sea and, second, if low-level clouds at altitudes below 700 hPa have been identified. Furthermore the segment should not contain any medium- or high-level clouds. The restriction to ocean areas, that is mainly to marine stratus and stratocumulus, is introduced since the yield of low-level cloud motion vectors over the continents is very small due to the scarcity of good tracers. This appears to be due to a lack of contrast over land that hampers tracking accuracy and, more importantly, a general lack of long-lived low-level cloud tracers over land (Shenk 1991). The winds are also affected by local orography and are not necessarily representative of the larger-scale wind field required for NWP models.

c. Wind vectors

The derivation of the displacement vector from successive VIS images is very similar to the operational tracking using the IR channel (Schmetz et al. 1993). A fully automated cross-correlation technique is applied to the high-resolution VIS images. As for the IR tracking, a target area of 32 $\times$ 32 VIS pixels is moved pixel by pixel in a search area of 96 $\times$ 96 VIS pixels in order to find the best match between successive images. Three successive images are used, which provides pairs of vectors. The automatic tracking for the generation of displacement vectors is applied to the four subsegments of the 32 $\times$ 32 IR pixel segment corresponding to areas of 32 $\times$ 32 VIS pixels. Typically about 750 out of 1863 IR segments located over oceans contain possible tracers. The 1863 segments refer to all ocean segments within the field of view of the satellite, including the small area over the Indian Ocean. The VIS tracking potentially provides a coverage with wind vectors that is four times as dense as the IR tracking; that is, the typical yield in VIS wind vectors is about 3000 vectors per production cycle.

d. Height allocation

The height allocation of a wind vector derived from tracking features in VIS images is based on the IR channel. A brightness temperature observed for the low-level cloud is interpolated into a short-term temperature forecast profile from the ECMWF. The observed brightness temperature also is corrected for the water vapor continuum absorption above cloud top (Schmetz 1986). This effect is typically an increase in temperature of the order of 1–2 K, which corresponds to a lowering of heights of up to 40 hPa.

The brightness temperatures used in assigning the height of a cloud tracer are taken from the multispectral analysis, which provides, for the sea segments under

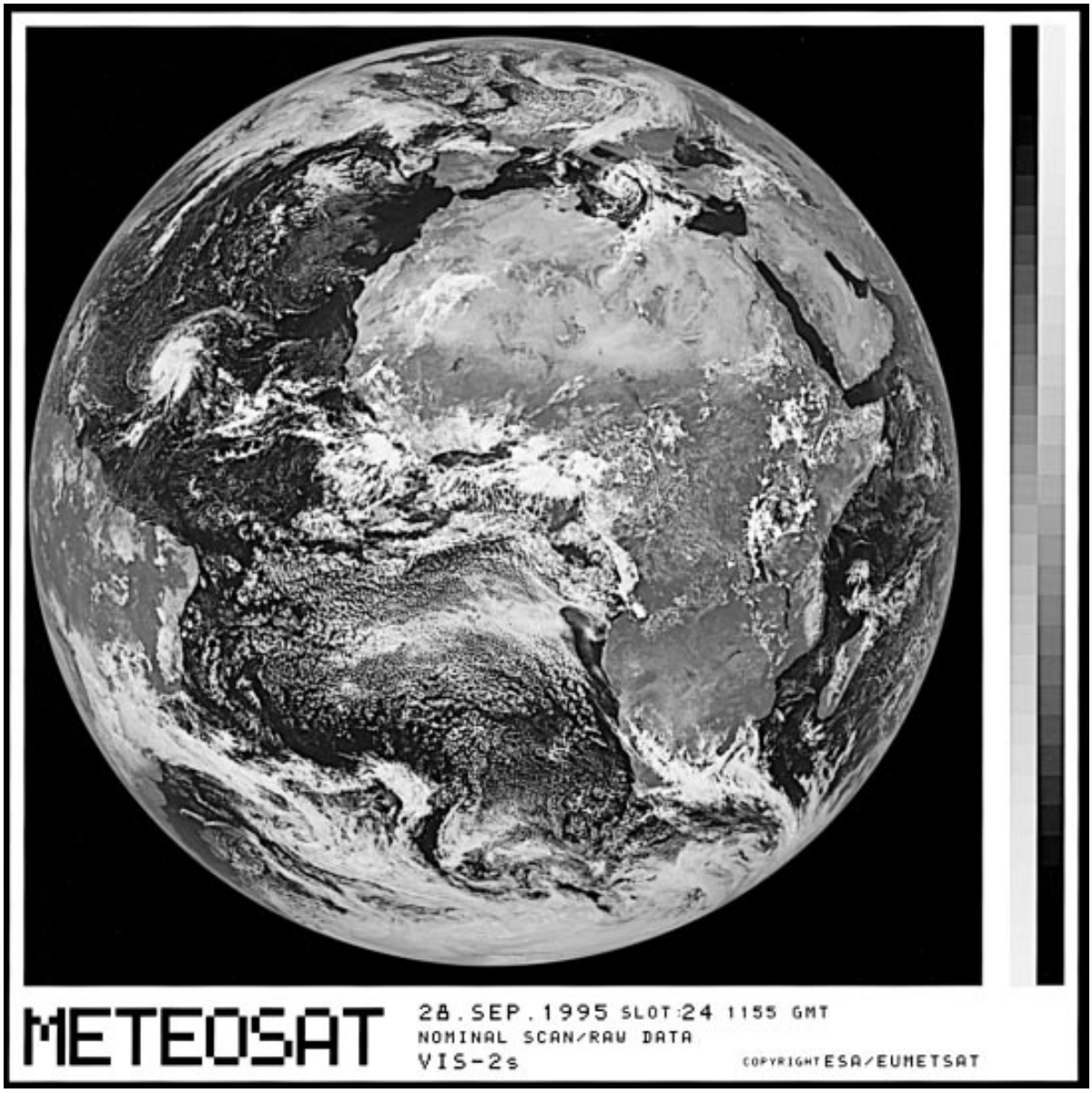

FIG. 1. Meteosat-5 full-resolution VIS for 28 September 1995, slot 24 (1130 UTC).

consideration, mean values for clear ocean and low cloud as well as standard deviations for the clusters identified in the histogram. Figure 3 shows the histogram of a typical ocean segment partially covered by clouds. Taking the mean value of the cloud cluster for the height assignment assigns the displacement vector to a mean cloud top. Although this is commonly done for medium- and high-level CMWs, a study by Hasler et al. (1979) clearly demonstrates that the approach is inappropriate for low-level clouds. They found, in a comparison of accurate aircraft winds with low-level satellite-tracked wind over the trade wind and subtropical high regions, that the cumulus-type marine clouds move at the same speed as the cloud-base-level winds. Since cloud-base temperature cannot be measured directly from space, a judicious estimation technique needs to be developed. Following the idea of Le Marshall et al. (1994), we infer cloud base T_{Base} from the histogram (Fig. 3) according to

$$T_{\text{Base}} = T_{\text{Cld}} - \sqrt{2}\sigma_{\text{Cld}}, \tag{1}$$

where T_{Cld} is the cluster mean temperature of the cloud cluster and σ_{Cld} is the standard deviation of the cloud cluster. It is assumed that the histogram can be fitted with two half Gaussians on either side of the cluster. The value $(2)^{1/2}\sigma_{\text{Cld}}$ is the point taken as cluster boundary, where the probability density function attains the value $1/e$. This cluster boundary is assumed to be the

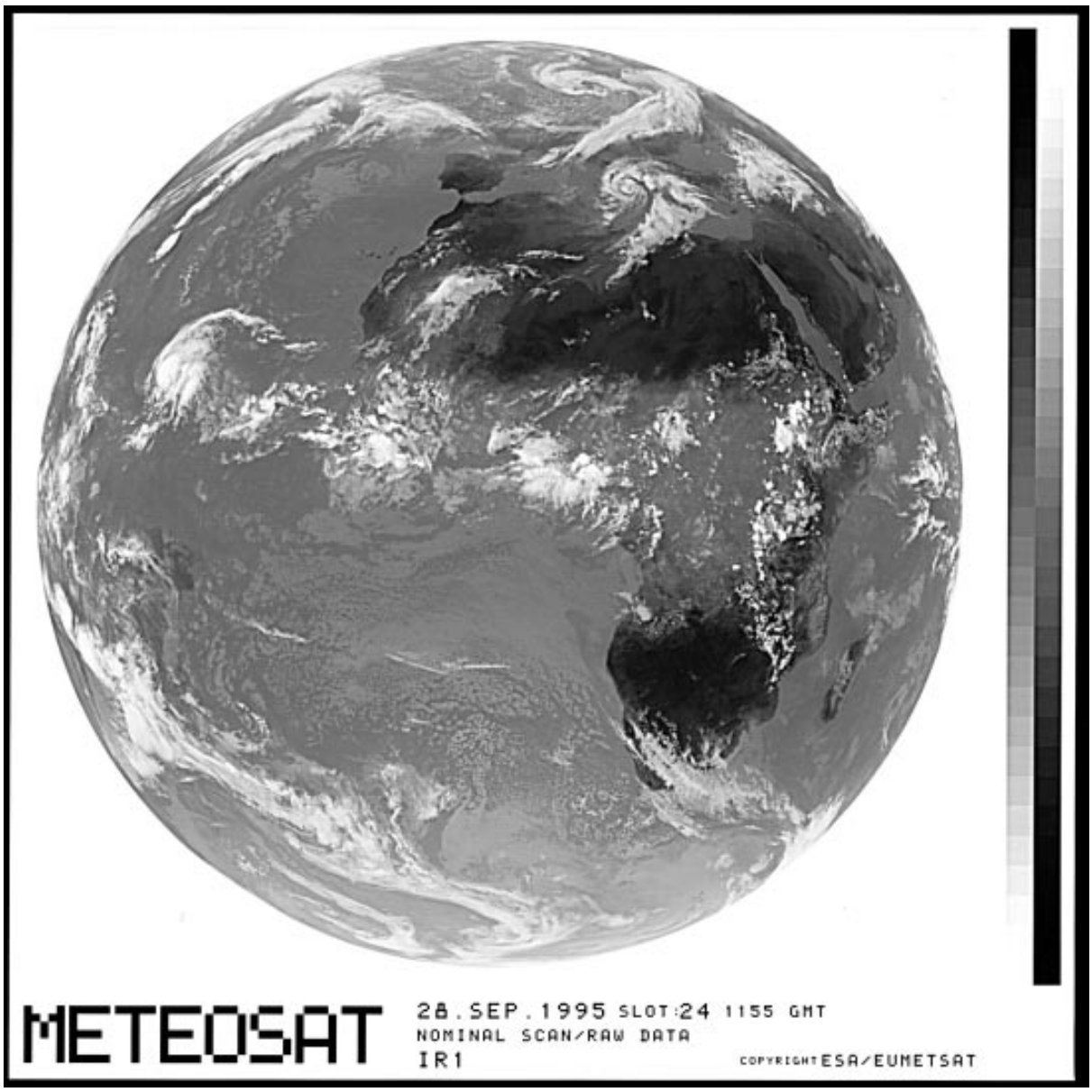

FIG. 2. Meteosat-IR image for 28 September 1995, slot 24 (1130 UTC).

cloud base. In agreement with Le Marshall et al. (1994), we find that lowering the height assigned to a low-level wind vector generally provides a better fit to an analysis.

e. Automatic quality control

The VIS CMWs are subject to several internal consistency checks described below and a final rough check against a short-term forecast of the wind field. The quality control is fully automatic and no manual intervention is performed, in contrast to the operational IR winds (Schmetz et al. 1993).

The first step in the automatic quality control is the symmetry check where a pair of vectors derived from the three successive images is checked for agreement. The internal consistency check considers a vector and its eight neighbors. A vector must have at least one neighbor with cloud-base heights within 20 hPa, wind directions within 30°, and wind speeds within 2 m s^{-1}. CMWs failing to satisfy one of the above criteria, as well as isolated vectors with no immediate neighbors, are rejected.

As an additional filter, a rough check against a short-term forecast is included. The purpose of that check is mainly to reject high-speed winds derived from semitransparent cirrus clouds that are falsely assigned to low levels when the semitransparency (Bowen and Saunders 1984; Schmetz et al. 1993) detection and correction

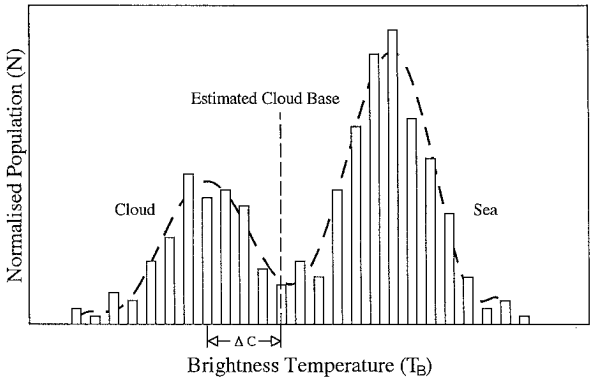

FIG. 3. Schematic diagram showing the histograms of brightness temperatures from a low-level cloud and clear ocean. The estimated cloud base is indicated.

failed. The check against the forecast is very rough indeed, since CMWs only are rejected if their vector difference against the forecast is larger than 75% of the forecast vector. More stringent checks would obviously increase the agreement between data and short-term forecast. This would come, however, at the expense of possibly rejecting good data in areas where the forecast is wrong. The forecast check was introduced as of 1 March 1995 and has effectively screened the above-mentioned outliers. Statistics concerning the forecast check are presented later in the section on results.

3. Results

Between June 1994 and November 1995, cloud motion winds from Meteosat full-resolution visible images (VIS-CMWs) were derived on a daily basis at 1100 UTC at the European Space Operations Centre (ESOC) and disseminated to ECMWF.

An example of the VIS-CMW product is provided in Fig. 4. A total of 2927 low-level ($\geq$700 hPa) VIS-CMWs was produced and disseminated to ECMWF for evaluation purposes. The example in Fig. 4 shows that the derived VIS-CMWs clearly depict the low-level flow over the marine stratocumulus regions. Smaller-scale wind features are also discernable. For comparison, Fig. 5 shows the corresponding low-level wind product from the IR tracking. Only 484 vectors were obtained and disseminated. Although the broad flow also is depicted in Fig. 5, the higher yield in vectors, as seen in Fig. 4, convincingly demonstrates the superior performance of the VIS tracking. It is notable that the VIS tracking yields about six times more winds than the IR tracking. Since at best four winds can be derived in an area of one IR wind, the factor of 6 cannot be explained just by the smaller templates used in the tracking. Rather the VIS images provide evidence that more clouds have been successfully tracked due to better contrast and resolution.

Since January 1995, two major software changes have been applied to the VIS-CMW retrieval algorithm. On 2 January 1995, the cloud-top-based height assignment scheme for low-level VIS-CMWs was replaced with the cloud-base-oriented height assignment approach as described above. It should be noted that the same change was applied to the operational IR winds. A second modification on 1 March 1995 enhanced the automatic quality control for the VIS-CMWs; that is, the local consistency check was supplemented with a rough check against the ECMWF wind forecast. Since then, the final quality check consists of two fully automatic steps.

The quality of the VIS-CMWs and the impact of the changes summarized above were routinely monitored by comparisons with collocated ECMWF forecast winds, since the number of rawindsonde stations in marine regions is too low to produce reasonable statistics. Therefore, statistics between VIS-CMWs and the first guess (6-h forecast, hereafter called FG) wind field of the ECMWF forecast model are used to show the improvements. Table 1 shows the speed and direction bias and standard deviations, respectively, between VIS CMW and first guess for the 2-month periods before (Nov–Dec 1994) and after (Jun–Jul 1995) the forecast check and the new height assignment were instituted. While the speed bias (observation minus first guess) reduces from 0.4 to 0.0 m s^{-1}, the standard deviation of the speed differences decreased from 2.6 to 2.1 m s^{-1}. Most notable is the reduction in the standard deviation of wind direction from 35.9° to 12.6°. It is noted that the comparison is largely improved without significantly altering the number of disseminated VIS-CMWs, which confirms that the first-guess check is a filter that only rejects a small number of gross outliers.

It is also interesting to put the performance of the VIS-CMWs into perspective by comparing it with satellite-tracked winds from other satellites and channels. Table 2 presents summary statistics of all the low-level CMWs received during a period between 28 August and 9 September 1995 at ECMWF, listed by satellite operator and channel. The quality of all low-level winds is similar, although Meteosat appears to perform slightly better in terms of direction as the standard deviation is somewhat lower. In that context, one should note that the U.S. GOES low-level CMWs are assigned to a fixed height of 900 hPa, and the Japanese GMS IR and VIS to 850 hPa. In this method each low-level cloud vector is assigned to pressure level corresponding to the cloud base temperature as computed from Eq. (1). A forecast profile is used to assign a temperature to a pressure. The overall quality of the high-resolution VIS-CMWs is similar to the other datasets, but the number of winds is significantly higher.

Here we should mention that as of 1 December 1995 satellite-tracked winds are produced operationally with a new hardware and software system at EUMETSAT (European Organisation for Meteorological Satellites). For the time being, VIS winds are produced only at a scale of the IR winds; however, a EUMETSAT high-

FIG. 4. Wind vectors derived from tracking clouds in high-resolution VIS images on 28 September 1995, 1130 UTC (see Fig. 1). A total of 2927 low-level vectors has been obtained.

resolution VIS wind product is now available and disseminated even five times per day for 0006, 0009, 0012, 0015, and 0018 UTC, respectively. These high-resolution VIS winds will be derived in a way as described in this paper.

4. Impact on the numerical weather prediction model at ECMWF

In order to evaluate the impact of the high-resolution VIS-CMW on the ECMWF forecast model, a data assimilation experiment, hereafter called VOPS, was performed from 24 August 1995 until 9 September 1995. During VOPS, VIS-CMWs were assimilated in the model in the same manner as the operational CMWs and, simultaneously, with operational, conventional, and other satellite observations. In order to assess the impact of the new data, the analysis and forecast fields of VOPS were compared to those of the operational scheme, hereafter called OPS, for the same period. The assimilation experiments were carried out using the optimal interpolation data assimilation scheme in operational use at the time.

The average impact of the VIS-CMW on the wind field analysis is presented in Fig. 6, which shows the rms wind vector difference at 850 hPa between the VOPS and the OPS together with the isotachs at 850 hPa. Over the complete area, the average change in the VOPS is 1–2 m s^{-1} (light stippled). The differences are most pronounced over the South Atlantic where the difference locally is more than 2 m s^{-1} (dark stippled), which corresponds to about 15%–20% of the mean wind speed.

The impact of VOPS on the 24-h forecasts is less pronounced than in the analyses shown in Fig. 6. However, the assimilation of the VIS-CMW produces a small positive impact, overall. Figure 7 presents the improvement in the 24-h forecast rms error between the VOPS and the OPS. Over some areas of the Atlantic, the VOPS rms error decreased by 0.5 m s^{-1} in comparison to OPS,

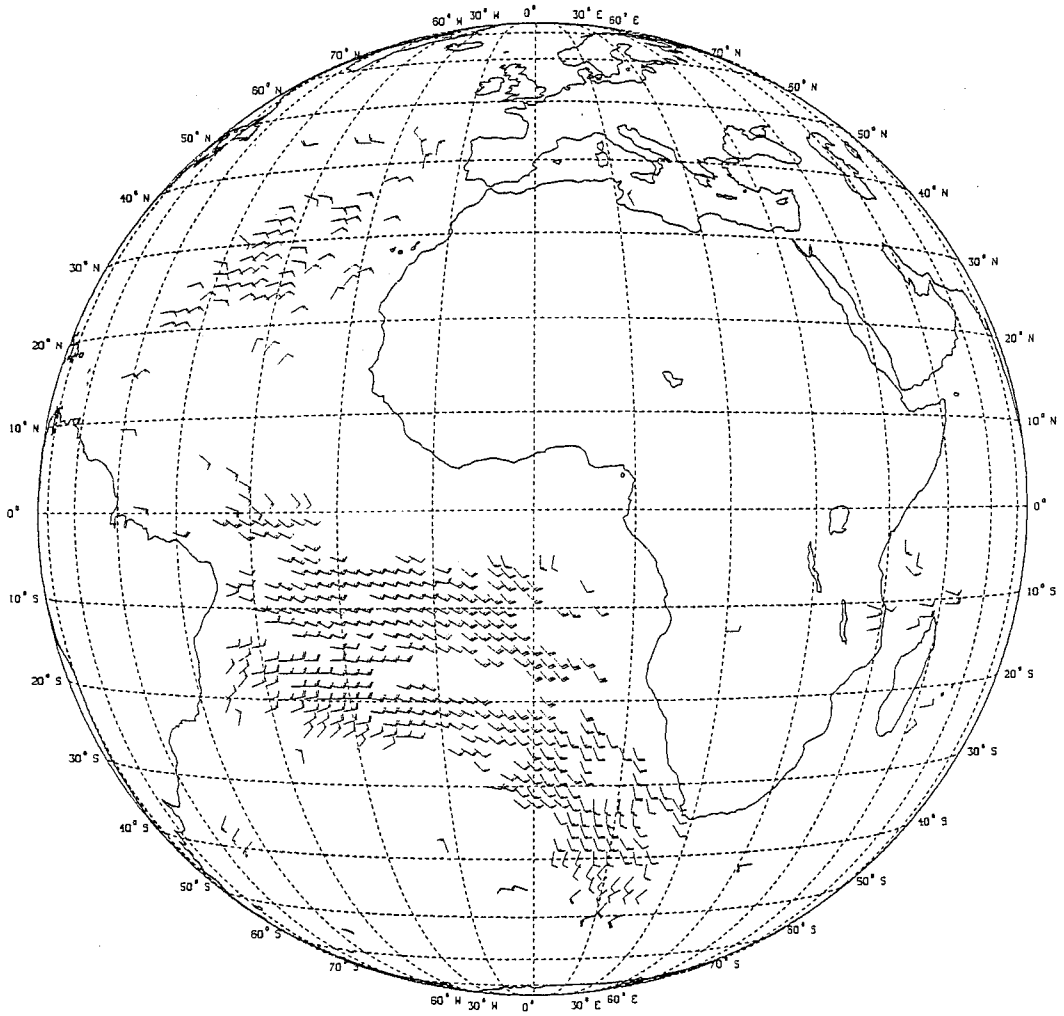

FIG. 5. As in Fig. 4 except that the wind vectors are derived from IR images (see Fig. 2). A total of 484 vectors has been obtained.

corresponding roughly to a 15% improvement. The evaluation of longer forecast periods (not shown) demonstrates that the impact of the VIS-CMW is progressively lost as the forecast period gets longer and, eventually, the effect on the medium range forecast is neutral.

It is also worthwhile to note that the differences between the VOPS and OPS wind fields for any particular day do not show significant features related to a particular synoptic situation. This might be due to the following facts. First, both the VOPS and the OPS already use the operational low-level IR-CMWs from Meteosat, which depict the gross low-level flow, though not to the detail discernible in the VIS-CMWs. Therefore, only

TABLE 1. Bias and standard deviation (std) between observation and first guess (FG) for the visible CMW at 1200 UTC before and after the changes in height assignment on 1 January 1995 and the introduction of the forecast check on 1 March 1995.

	Speed (m s^{-1})		Direction (°)		FG mean speed	
OBS-FG	Bias	Std	Bias	Std	(m s^{-1})	No. obs
Nov–Dec 94	0.4	2.6	−0.9	35.9	8.3	139 610
Jun–Jul 95	0.0	2.1	−1.2	12.6	9.4	137 074

TABLE 2. Bias and standard deviation (std) between observation and first guess (FG) for the low-level CMWs at 1200 UTC received at ECMWF for different satellites and channels during the period 24 August 1995–9 September 1995.

	Speed (m s^{-1})		Direction (°)		FG mean speed	
	Bias	Std	Bias	Std	(m s^{-1})	No. obs
Meteosat VIS	0.0	1.9	0.2	16.1	9.5	68 349
Meteosat IR	0.1	1.9	0.1	15.1	10.1	22 724
GOES IR	−0.5	2.0	−0.2	21.4	7.8	29 091
GMS IR	0.2	2.3	0.0	24.2	8.3	13 643
GMS VIS	0.4	2.2	0.3	24.5	8.4	11 837

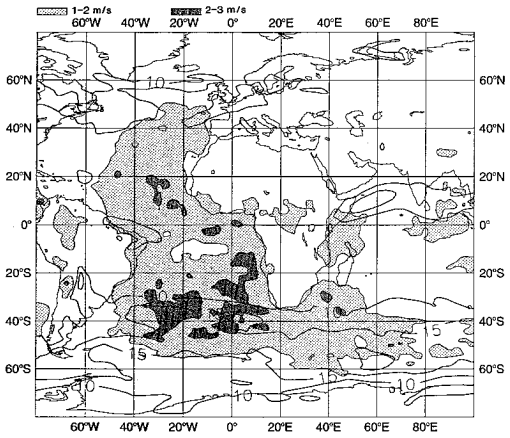

FIG. 6. Mean rms vector difference between VOPS and OPS analyses, respectively, at 850 hPa from 24 August 1995 to 9 September 1995.

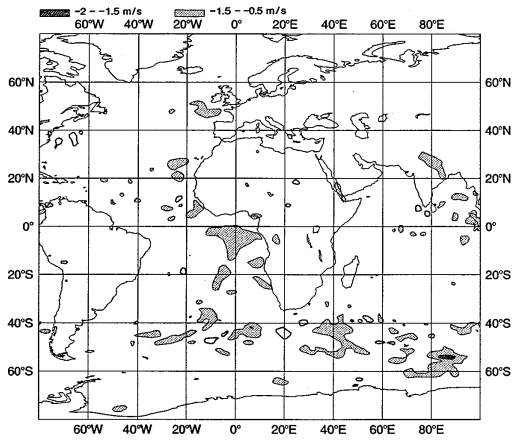

FIG. 7. Mean difference of the 24-h forecast (rms) error between VOPS and OPS for the period 24 August 1995 to 9 September 1995. The verifying analysis is the VOPS one; contour interval is shaded below -0.5 m s^{-1}, indicating an improved VOPS forecast.

the impact of the additional information contained in the high-resolution VIS-CMWs is observed. Second, the prevailing tropical circulation during the period of the experiment, namely the development of tropical storms, is well described by the ECMWF model. This is particularly evident during 29 August 1995, when many VIS-CMWs were available in the vicinity of Tropical Storm Luis (Fig. 8). Despite the lack of operational low-level CMWs, the analysis of the model already located and depicted correctly the storm and, consequently, little was left for improvement. It is to be expected that in other cases the VIS-CMWs would have a larger impact if a situation is analyzed using those additional data, at times when the forecast model performance is poor.

The forecast experiments described above do not assimilate the wind measurements from the *ERS-1* (*European Remote Sensing Satellite-1*) scatterometer, and, therefore, this dataset is considered as an independent source of information for verification purposes. While the low-level CMWs are representative of a cloud layer located between the surface and 700 hPa, the scatterometer senses surface winds. A direct comparison of the two, therefore, is not appropriate. However, when CMWs are assimilated, the resulting FG wind fields at the surface are affected by the low-level flow as captured by the CMWs, and the FG surface wind field can then be compared with the scatterometer data retrieved at ECMWF (Gaffard and Roquet 1995; Stoffelen and Anderson 1997).

Results from the comparison of *ERS-1* winds against the first guess for the VOPS and the OPS can be summarized as follows. Improvements in the direction standard deviation between FG wind at 10 m and the scatterometer winds are observed, with the largest improvement of 0.5° in the Southern Hemisphere. This is also consistent with the expectation that the impact of the high-resolution VIS winds is largest in the Southern Hemisphere since there the quality of the forecast generally is inferior to Northern Hemisphere forecasts. The minute magnitude of the impact of VIS-CMWs in VOPS is explained by the fact that the OPS forecast already contains low-level IR CMWs and thus contains information on winds inferred from the movements of low-level clouds. However, one can conclude that the small but positive impact of high-resolution VIS CMWs is encouraging since it has been obtained without any data-specific tuning of quality control and assimilation procedure, which is usually required when data from a new source is first assimilated.

5. Conclusions

Winds are derived from tracking clouds in high-resolution Meteosat VIS images, with a template size of 32×32 VIS pixels corresponding to about 80 km $\times$ 80 km at the subsatellite point, a level of resolution that is four times better than the corresponding IR winds. The winds have been experimentally derived at the European Space Operations Center (ESOC) once per day (1100 UTC) from July 1994 until November 1995. The utilization of the VIS channel typically increases by a factor of 6 the number of low-level CMWs compared to those yielded by the IR only. This is in part due to the smaller template size used in the VIS tracking and in part due to better contrast and spatial resolution. The smaller template size and higher yield provides for a better description of the circulation, including features of smaller scales, as evidenced by a comparison of Figs. 4 and 5.

A comparison of IR low-level wind fields from different geostationary satellites with the first guess of the ECMWF forecast model shows that the winds derived from the tracking of clouds in high-resolution Meteosat VIS images have a quality comparable to IR low-level cloud motion winds. Generally, the standard deviation between FG wind speed and observation is around 2 m s^{-1}.

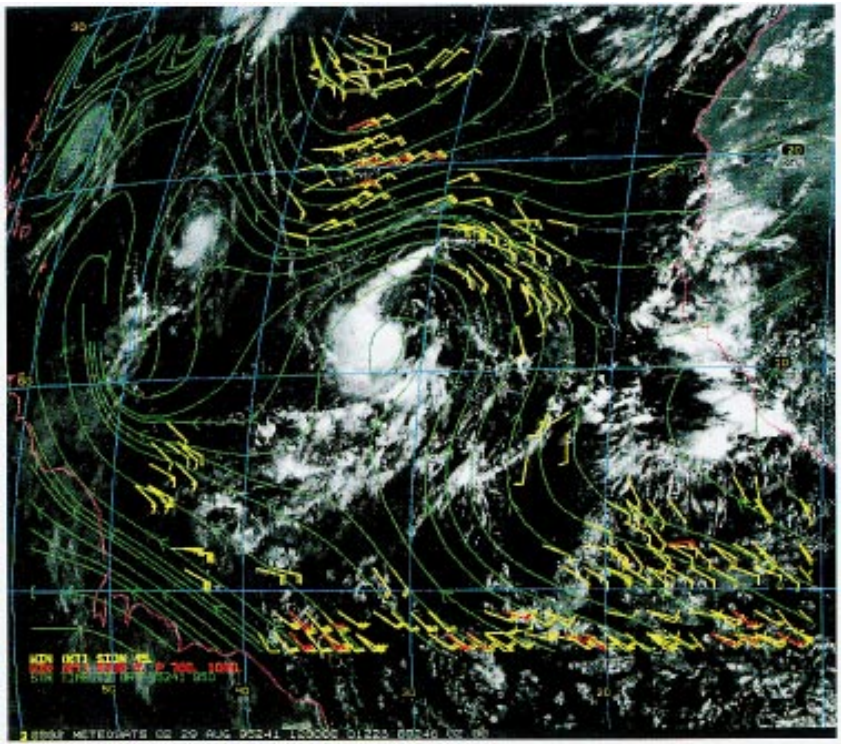

FIG. 8. Meteosat visible image of Tropical Storm Luis on 29 August 1995. The yellow wind flags are the visible CMW; the red one the operational low-level infrared CMW. The green contour represents the 850-hPa streamlines of the OPS analyses. The reported position of the storm center was 12.0°N, 32.1°W.

The impact of the VIS-CMWs has been tested with a data assimilation experiment at ECMWF. The operational forecast system, which includes low-level IR winds, has been compared with forecasts also encompassing VIS-CMW. The inclusion of the latter has led to mean changes of up to 2 m s^{-1} of the vector rms in the analysis over the South Atlantic. The impact on a 24-h forecast is positive and produces a reduction of the vector rms of the order of 0.5 m s^{-1} or 15% over some areas of the Atlantic Ocean. Improvements are most pronounced in the South Atlantic. A comparison of the model FG wind field at 10 m using the VIS-CMW with independent scatterometer winds from *ERS-1* confirms the small but consistent improvement.

ECMWF has recently changed its data assimilation to a three-dimensional variational analysis (3DVAR). It is anticipated that the impact of CMWs in NWP will be greater using these more optimal analyses, and experiments are under way to demonstrate this.

A drawback of VIS winds is their limitation to daytime satellite observations, which also implies a migration of the processing area for VIS winds over the satellite field of view throughout a day. The high-resolution VIS winds presented in this study have been derived at ESOC on an experimental basis between July 1994 and November 1995. Winds were disseminated to ECMWF for validation in their data assimilation system. On 15 November 1995 the derivation of satellite tracked winds from Meteosat was transferred from ESOC to EUMETSAT. The satellite operation and product derivation at EUMETSAT are both based on a new concept and new systems that differ from the ones previously used at ESOC. In the beginning the new system at EUMETSAT did not provide winds from high-resolution VIS images; however, in view of the success of the experimental work at ESOC, the derivation of a high-resolution VIS wind product commenced at EUMETSAT in 1996 with a method as described in this paper.

Acknowledgments. Thanks are due to three referees for their thorough reviewing, which helped to improve this paper.

REFERENCES

Bowen, R. L., and R. N. Saunders, 1984: The semitransparency correction as applied operationally to Meteosat infrared data: A remote sensing problem. *Eur. Space Agency J.,* **8,** 125–131.

Gaffard, C., and H. Roquet, 1995: Impact of the ERS-1 scatterometer wind data on the ECMWF 3D-Var assimilation system. ECMWF Tech. Memo. 217, 22 pp.

Hasler, A. F., W. C. Skillman, and W. E. Shenk, 1979: In situ aircraft

verification of the quality of satellite cloud winds over oceanic regions. *J. Appl. Meteor.*, **18,** 1481–1489.

Holmlund, K., 1993: Operational water vapour wind vectors from Meteosat imagery data. *Proc. Second Int. Wind Workshop*, Tokyo, Japan, EUMETSAT, 77–84.

Hubert, L. F., and L. F. Whitney Jr., 1971: Wind estimation from geostationary satellite pictures. *Mon. Wea. Rev.*, **99,** 665–672.

Kelkar, R. R., and A. V. R. K. Rao, 1992: Extraction of quantitative meteorological information from INSAT imagery. *J. Meteor. Soc. Japan*, **70,** 551–561.

Kelly, G., 1992: Satellite observations for global monitoring. *Adv. Space Res.*, **7,** 263–275.

Laurent, H., 1993: Wind extraction from Meteosat vapor channel image data. *J. Appl. Meteor.*, **32,** 1124–1133.

Leese, L., S. Novak, and B. Clark, 1971: An automated technique for obtaining cloud motion from geosynchronous satellite data using cross correlation. *J. Appl. Meteor.*, **10,** 118–132.

Le Marshall, J., 1994: An operational system for generating cloud drift winds in the Australian region and their impact on numerical weather prediction. *Wea. Forecasting*, **9,** 361–370.

Merrill, R. T., W. P. Menzel, W. Baker, J. Lynch, and E. Legg, 1991: A report on the recent demonstration of NOAA's upgraded capability to derive cloud motion satellite winds. *Bull. Amer. Meteor. Soc.*, **72,** 372–376.

Nieman, S., J. Schmetz, and W. P. Menzel, 1993: A comparison of several techniques to assign heights to cloud tracers. *J. Appl. Meteor.*, **32,** 1559–1568.

Radford, A., 1989: Monitoring of cloud-motion winds at ECMWF. *Proc. ECMWF/EUMETSAT Workshop: The Use of Satellite Data in Operational Numerical Weather Prediction: 1989–1993*, Vol. I-I, 249–262.

Reed, R. A., A. Hollingsworth, W. A. Heckley, and F. Delsol, 1988: An evaluation of the ECMWF operational system analyzing and forecasting tropical easterly wave disturbances over Africa and the tropical Atlantic. *Mon. Wea. Rev.*, **116,** 824–865.

Rodgers, E., R. C. Gentry, W. Shenk, and V. Oliver, 1979: The benefits of using short interval satellite images to derive winds for tropical cyclones. *Mon. Wea. Rev.*, **107,** 575–584.

Schmetz, J., 1986: An atmospheric-correction scheme for operational application to METEOSAT infrared measurements. *Eur. Space Agency J.*, **10,** 145–159.

——, K. Holmlund, J. Hoffman, B. Strauss, B. Mason, V. Gaertner, A. Koch, and L. van de Berg, 1993: Operational cloud-motion winds from Meteosat infrared images. *J. Appl. Meteor.*, **32,** 1206–1225.

Shenk, W. E., 1991: Suggestions for improving the derivation of winds from geosynchronous satellites. Operational Satellites: Sentinels for the monitoring of climate and global change. *Global Planet. Change*, **4,** 165–171.

Stewart, T. R., C. M. Hayden, and W. L. Smith, 1985: A note on water vapor wind tracking using VAS data on McIDAS. *Bull. Amer. Meteor. Soc.*, **66,** 1111–1115.

Stoffelen, A., and D. Anderson, 1997: Ambiguity removal and assimilation of scatterometer data. *Quart. J. Roy. Meteor. Soc.*, in press.

Thoss, A., 1992: Cloud motion winds, validation and impact on numerical weather forecast. *Proc. Workshop on Wind Extraction from Operational Meteorological Satellite Data*, Washington, DC, EUMETSAT, 105–112.

Tomassini, C., 1981: Objective analysis of cloud fields. *Proc. Satellite Meteorology of the Mediterranean*, Erice, Italy, ESA, 73–78.

Uchida, H., 1992: Height assignment for GMS high-level cloud motion winds. *Proc. Workshop on Wind Extraction from Operational Meteorological Satellite Data*, Washington, DC, EUMETSAT, 27–32.

——, T. Oshima, T. Hamada, and S. Osano, 1991: Low-level cloud motion wind field estimated from GMS short interval images in typhoon vicinity. *Geophys. Mag.*, **44,** 37–50.

Velden, C. S., C. M. Hayden, W. P. Menzel, J. L. Franklin, and J. S. Lynch, 1992: The impact of satellite-derived winds on numerical hurricane track forecasting. *Wea. Forecasting*, **7,** 107–118.